Reduction of Eddy-Current Losses in Fractional-Slot Concentrated-Winding Synchronous PM Machines

Gilsu Choi and Thomas M. Jahns, *Fellow, IEEE*

Department of Electrical and Computer Engineering, University of Wisconsin–Madison, Madison, WI 53706 USA

This paper presents the results of an investigation focused on the rotor eddy-current losses of a permanent magnet (PM) synchronous machine that is equipped with fractional-slot concentrated windings (FSCWs). Major spatial harmonics that induce the most significant rotor eddy-current losses are identified and evaluated. Time-stepped finite-element analysis results are presented to compare the predicted losses in the proposed FSCW-PM machine designs. It is shown that the lowest total eddy-current losses in the rotor core and magnets are achieved by introducing flux barriers into the rotor back iron along the *d*-axis.

***Index Terms*— Eddy-current loss reduction, fractional-slot concentrated windings (FSCWs), magnetomotive force (MMF) harmonics, permanent magnet (PM) machines.**

I. Introduction

SYNCHRONOUS permanent magnet (PM) machines equipped with fractional-slot concentrated windings (FSCWs) offer high torque/power density and other attractive performance characteristics [1]. However, one major drawback is their high spatial magnetomotive force (MMF) harmonics in the air gap that are caused by the stator phase currents. These harmonics asynchronously rotate with the rotor, yielding large eddy-current losses in the rotor core and magnets during high-speed operation [2]. Some techniques to reduce the MMF harmonic amplitudes have been published [3]–[5], but they often require significant changes in the machine designs that increase their cost and complexity. The impact of the rotor yoke on the rotor losses was investigated in [6]. However, the technique proposed in [6] was demonstrated for a surface PM machine only, and no accompanying technical details have been provided to explain the technique.

The objective of this paper is to reduce the sub-harmonic components of the stator armature reaction field by minimizing the flux flowing through the rotor back iron. First, analytical insights into the rotor eddy-current losses of FSCW-PM machines are developed. Next, major spatial harmonics that have the most significant impact on the rotor eddy-current losses of FSCW-PM machines are identified. Finally, finite-element (FE) results are presented to compare the predicted losses in the machine core and magnets of FSCW-PM machines for three different configurations: 1) completely removed rotor back iron (yokeless); 2) slits are introduced into the rotor back iron as flux barriers along the d-axis (d slit); and 3) slits are introduced along the q-axis (q slit). It is shown that the lowest rotor core losses are achieved by adopting the yokeless design, while the lowest total rotor losses are achieved with the d slit design.

II. MMF Harmonic Spectra in FSCW-PM Machines

It is well known that the FSCW-PM machines exhibit higher spatial harmonic components in the stator MMF distribution than the corresponding integral-slot winding PM machines. Using the analytical expressions in [7], spatial harmonic components developed in FSCW-PM machines for each of the slot/pole configurations with double-layer (DL) and single-layer (SL) windings are defined as follows:

$$\text{For DL windings} \begin{cases} (2n-1)\cdot t & N_s/t \text{ is even} \\ n\cdot t & N_s/t \text{ is odd} \end{cases}$$

$$\text{For SL windings} \begin{cases} (2n-1)\cdot t & N_s/t \text{ is even } \& \ N_s/2t \text{ is even} \\ n\cdot t & N_s/t \text{ is even } \& \ N_s/2t \text{ is odd} \\ n\cdot t/2 & N_s/t \text{ is odd } \& \ t \text{ is even} \end{cases} \quad (1)$$

where N_s is the number of stator slots, p is the number of pole pairs, t is the greatest common divisor between N_s and p, and n is any positive integer.

Of the MMF spatial harmonics, the stator slot harmonics are particularly important, because these harmonics are characterized by the same winding factor as the main synchronous harmonic, causing high rotor losses, especially when the harmonic component is rotating backward [7]. The orders of the stator slot harmonics are $h = k \cdot Ns \pm p$ for the spatial harmonics and $h = k \cdot Ns/p$ for the time harmonics, where k is a non-negative integer.

Fig. 1 shows the per-unit amplitudes of the current-induced air-gap MMF harmonic components in a 12-slot/10-pole FSCW-PM machine, highlighting the presence of the sub-harmonic of order $h = 1$. The amplitude of the $h = 1$ spatial sub-harmonic significantly increases when the windings are switched from the DL to the SL. Due to its longer wavelength,

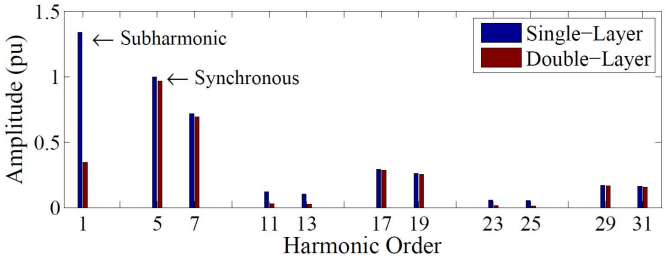

Fig. 1. Stator current MMF spatial harmonic spectra of a 12-slot/10-pole FSCW-PM machine with SL and DL winding configurations.

Manuscript received November 6, 2015; accepted January 3, 2016. Date of publication January 12, 2016; date of current version June 22, 2016. Corresponding author: G. Choi (e-mail: gchoi4@wisc.edu).

Color versions of one or more of the figures in this paper are available online at http://ieeexplore.ieee.org.

Digital Object Identifier 10.1109/TMAG.2016.2517144

TABLE I
HARMONIC CHARACTERISTIC PROPERTIES OF A 12-SLOT/10-POLE FSCW-PM MACHINE WITH SL WINDINGS

Harmonic order		k_{wh}	Freq. (kHz)	Rotating direction
Spatial	Seen by rotor			
1	6	0.259	1	BWD
5	0 (DC)	0.966	0 (DC)	FWD
7	12	0.966	2	BWD
11	6	0.259	1	FWD
13	18	0.259	3	BWD
17	12	0.966	2	FWD
19	24	0.966	4	BWD

the flux caused by the sub-harmonic MMF flows through the rotor and stator back iron, increasing the saturation level in the core and corresponding losses. In addition to the case with SL windings, the sub-harmonics are generally higher than the fundamental harmonic when the number of poles is higher than the number of slots [7].

Each spatial harmonic asynchronously rotates with the fundamental frequency and its frequency depends on the harmonic order. First, the mechanical angular speed of the hth MMF harmonic in the stator reference frame, $\omega_{\rm sh}$, can be written as

$$\omega_{\rm sh} = 2\pi f_s(\pm 1/h) \tag{2}$$

where f_s is the fundamental frequency, and $\pm$ sign is $+$ when the hth harmonic wave is rotating forward and $-$ for backward rotating wave with respect to the rotor. The sign can be determined for a three-phase machine as follows:

$$\text{sign} = \frac{2}{3} \cdot \sin[(1 + h - p) \cdot (2\pi/3)]. \tag{3}$$

Next, the angular speed of hth MMF harmonic in the rotor reference frame results in

$$\omega_{\rm rh} = 2\pi f_s(\pm 1/h - 1/p). \tag{4}$$

Finally, the corresponding harmonic frequency of the hth MMF harmonic seen by the rotor is obtained as follows:

$$f_{\rm rh} = f_s|\pm h/p - 1|. \tag{5}$$

Table I presents the harmonic order, harmonic winding factor $k_{\rm wh}$, rotation direction, and frequency of each harmonic as seen by the rotor at the peak speed of 10 000 r/min for a 12-slot/10-pole FSCW-PM machine with SL windings.

III. ROTOR EDDY-CURRENT LOSSES IN FSCW-PM MACHINES

A. Rotor Core Eddy-Current Losses

In FSCW-PM machines operating at high speeds, minimizing rotor losses is more important because of the challenge associated with heat removal from a rotating object as well as demagnetization risks. Rotor eddy-current losses are the dominant losses in high-speed FSCW-PM machines. An expression for these rotor core eddy-current losses incorporating all harmonic effects is provided as follows [8]:

$$P_{\rm eddy} = k_e \sum_{h\geq 1} f^2 B^2 = k_e f_h^2[|hB_{\rm rh}|^2 + |hB_{\rm th}|^2] \tag{6}$$

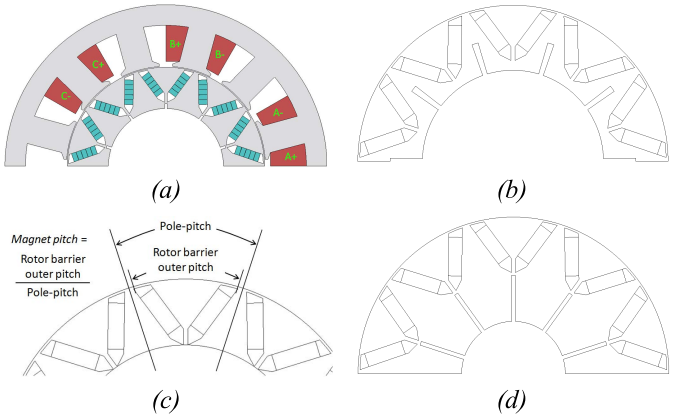

Fig. 2. Cross-sectional views of the baseline FSCW-IPM machines. (a) d slit. (b) q slit. (c) Yokeless. (d) d slit 2.

where f_h is the hth harmonic frequency, $B_{\rm rh}$ and $B_{\rm th}$ are the amplitudes of the hth radial and tangential flux density harmonics, respectively, and k_e is the eddy-current coefficient.

As shown in (6), the rotor core eddy-current losses are proportional to the square of harmonic flux density. The harmonic components are induced due to a combination of slotting effects, spatial harmonics attributable to the stator windings, and time harmonics due to PWM switching. Of these sources, the spatial harmonics are dominant in determining the rotor eddy-current losses in interior PM (IPM) machines [8]. In general, the rotor losses are proportional to the specific wavelength, harmonic order, and winding factor squared of order h. The impact of higher-order harmonics is often offset by the air gap that acts as a low-pass filter [7]. As a result, the sub-harmonic and the first slot harmonics ($h = 1, 7, 17$) are dominant in terms of rotor core eddy-current losses in the 12-slot/10-pole FSCW-PM machine with SL windings. This result is consistent with the FE results, as shown in Fig. 3.

B. Magnet Eddy-Current Losses

Since the magnet loss density also depends on the square of harmonic winding factor, the impact of the sub-harmonic MMF on the magnet eddy-current losses is not necessarily high. The magnet losses can be very high if there is a sub-harmonic that is also a stator slot harmonic [7]. In general, the slot harmonics have a significant impact on the magnet eddy-current losses.

IV. ROTOR LOSS MINIMIZING DESIGN APPROACH

A. Baseline FSCW-IPM Machines

As described in Section I, three different rotor configurations are proposed to minimize the impact of sub-harmonic MMF in the 12-slot/10-pole FSCW-IPM machine. Fig. 2(a)–(c) shows the cross sections of the three machine configurations. Fig. 2(d) shows the second d slit design (d slit 2) that accounts for the impact of a smaller rotor inner diameter due to the consideration of the shaft diameter. The number of circumferential magnet segments for all of the baseline designs is set to 5, as shown in Fig. 2(a).

The designs in Fig. 2(a) and (b) introduce additional magnetic reluctance into the rotor back iron, so that the MMF sub-harmonic flux is suppressed. In Fig. 2(c), the rotor back iron is

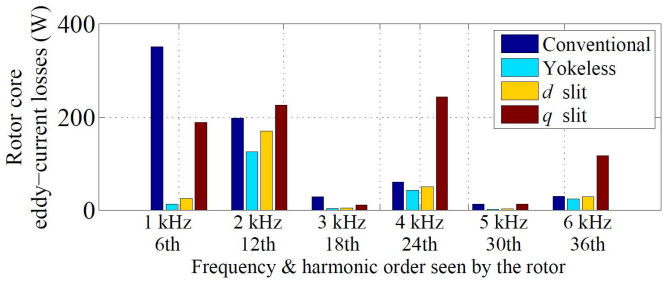

Fig. 3. FE-calculated harmonic spectra of the rotor core eddy-current losses at 10 000 r/min for the baseline machines ($I_{\text{rms}} = 100$ A and $\gamma = 85°$).

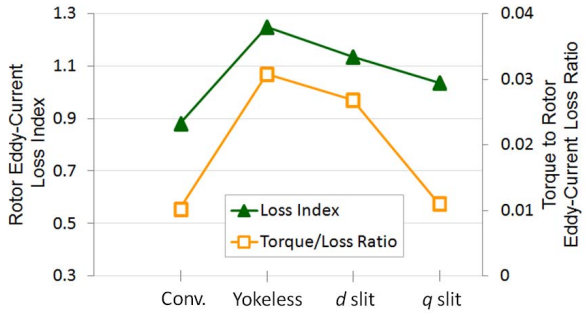

Fig. 4. FE-calculated rotor eddy-current losses for the baseline machines versus rotor eddy-current loss index at 10 000 r/min.

completely removed to achieve the maximum suppression of the MMF sub-harmonic flux. FE-calculated rotor core losses of the four baseline machines under open-circuit conditions are almost the same, indicating that the proposed design approach has minimal impact on the rotor losses due to slotting effects alone. Compared with the past work in [3]–[5], the advantages of the proposed configurations are their simplicity and flexibility.

B. Rotor Core Eddy-Current Loss Index

Since the magnet losses can significantly be reduced by segmenting the magnets [9], it is reasonable to first minimize the rotor core losses at the maximum operating speed.

Fig. 3 shows the FE-calculated harmonic spectra of the rotor core eddy-current losses at 10 000 r/min for the baseline machines, demonstrating that the majority of the losses are created by the first two time harmonic terms of frequency $f = 1$ and 2 kHz which correspond to the spatial harmonics of order $h = 1$, 7, 11, and 17. Using the dominant spatial harmonics to represent the rotor core eddy-current losses that are identified in Fig. 3, a new rotor core eddy-current loss index metric for the 12-slot/10-pole FSCW-IPM machines is defined as

$$\text{Rotor core eddy} - \text{current loss index} = \frac{B_{\text{fund}}}{\sum_{h=1,7,17} B_h}. \quad (7)$$

The loss index in (7) is the ratio of the fundamental flux density to the sum of major loss-inducing harmonic flux densities, reflecting the ratio of the output torque to the rotor core eddy-current losses. Fig. 4 shows the loss index values overlaid with the FE-calculated ratio of output torque to the rotor eddy-current losses, showing a very good correlation

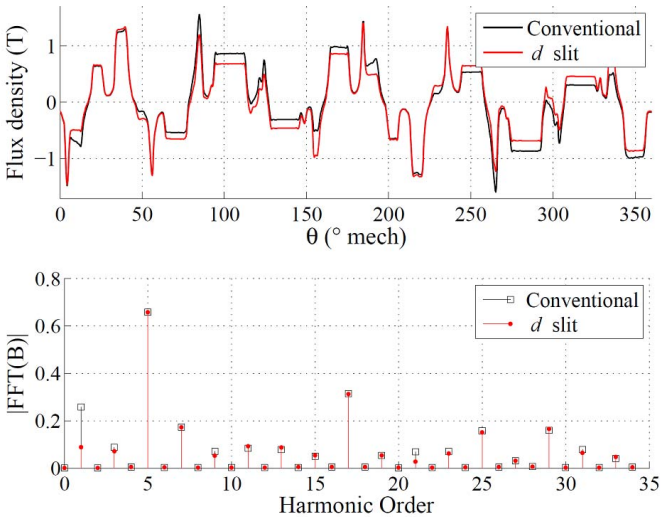

Fig. 5. Radial air-gap flux density versus angular position (top) and spatial harmonic spectrum (bottom) for the conventional and d slit designs at 10 000 r/min ($I_{\text{rms}} = 100$ A and $\gamma = 85°$).

between the loss index and torque-to-rotor loss ratio. This loss index makes it possible to rapidly calculate the estimates of the rotor core eddy-current losses during the design process.

The optimal depth and width of slits for minimum rotor core losses are found by applying the FE-calculated air-gap flux density values to (7). An investigation reveals that the rotor losses decrease as both the depth and the width of the slits increase. Therefore, the limiting factor for the design of d slit is decided by the structural integrity of the rotor laminations. Rotor losses for the q slit design are always higher than for the d slit design regardless of the shape of slit.

V. FE Analysis Results

A. Stator and Rotor Core Eddy-Current Losses

Fig. 5 shows the FE-calculated radial air-gap flux density as a function of angular rotor position and the corresponding harmonic spectra for both the conventional and d slit machines, clearly showing the reduction of the $h = 1$ sub-harmonic by 66% in the d slit machine. This leads to a significant reduction of rotor eddy-current losses for the d slit design, as shown in Fig. 3. Further reduction of the sub-harmonic and rotor losses is observed with the yokeless design.

Fig. 6 shows the results of FE analysis calculating the magnetic flux lines in the conventional and d slit machines, highlighting the reduction of saturation level in the stator and rotor back iron. This results in the reduction of both the stator and rotor core losses in the d slit machine, as shown in Fig. 7.

Fig. 7 provides a summary of the FE-calculated losses in different parts of the machine compared for the four designs during deep flux-weakening operation. As expected, stator and rotor core losses are the lowest for the yokeless design, followed by the d slot design. Since the sub-harmonic is not completely eliminated with the flux barriers in the q-axis, the core losses are generally higher in the q slit design. In addition, rotor core losses in the q slit design are aggravated by the long slits in the q-axis that elevate the saturation level in the rotor q-axis.

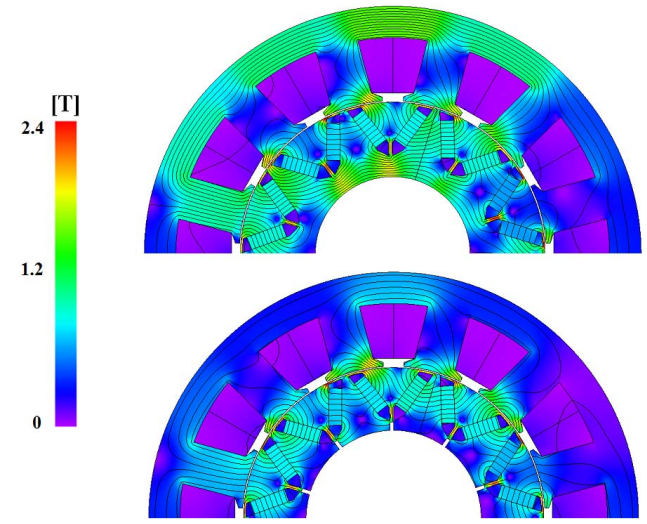

Fig. 6. Magnetic flux lines in the conventional (top) and d slit (bottom) designs at 10 000 r/min ($I_{\rm rms} = 100$ A and $\gamma = 85°$).

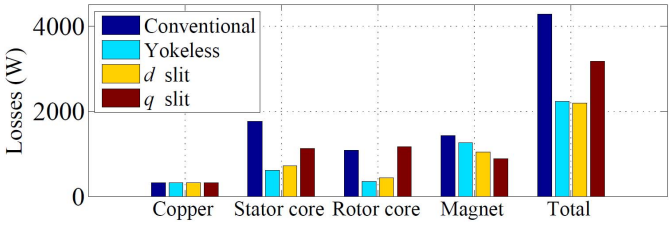

Fig. 7. FE-calculated total losses of the baseline machines at 10 000 r/min ($I_{\rm rms} = 100$ A and $\gamma = 85°$).

B. Rotor Magnet Eddy-Current Losses

Fig. 7 shows that the magnet losses are the lowest in the q slit design. This is because of the flux barriers in the q-axis that convert some loss-inducing high-order harmonics to more benign harmonics by altering the direction of the harmonic flux. Although the yokeless design exhibits the lowest total core losses, it has a potential issue with rotor structural integrity as well as elevated magnet losses.

In contrast, the d slit design has the lowest total losses. Rotor losses are reduced by 41% and stator losses by 60% in the d slit design during operation at maximum speed flux-weakening without degrading either the average torque or the torque ripple. Further loss reduction is possible by increasing the number of magnet segments in the axial direction [9]. The loss reduction is also lower at rated speed (3800 r/min). However, the efficiency in this operating region is typically very high (>96%).

C. Impact of Magnet Pitch Variation

Although the result is not shown here, the impact of magnet pitch, where its definition is shown in Fig. 2(c), on the machine losses has been studied using the FE analysis. FE results reveal that there is a decreasing trend in the rotor core losses as the magnet pitch increases from 0.85 to 1. This is because the amount of spatial flux harmonics that penetrate through the rotor q-axis is reduced with an increase in magnet pitch. However, there is also an increasing trend in the stator core loss and torque ripple with increasing magnet pitch due to the change in rotor MMF harmonics. In addition, magnet losses also increase with increase in magnet pitch. Therefore, a magnet pitch ratio of 0.92 has been chosen based on a desire to minimize total losses and torque ripple.

D. Impact of Shaft Diameter

As explained previously, the impact of a smaller rotor inner diameter due to the consideration for shaft diameter has been investigated using the FE analysis. Assuming a shaft diameter of 57 mm and a corresponding increased rotor back iron area, as shown in Fig. 2(d), the total losses increase by 16%.

VI. Conclusion

This paper presents a promising technique to reduce the eddy-current losses in FSCW-PM machines that have significant sub-harmonic MMF components by introducing magnetic flux barriers into the rotor back iron. A convenient loss index has been developed to provide rapid estimates of rotor eddy-current losses during the design process.

It has been shown that the lowest total eddy-current losses in the rotor core and magnets are achieved by introducing flux barriers into the rotor back iron along the d-axis, while the lowest total core losses are achieved when the rotor back iron is completely removed. On the other hand, the magnet losses are the lowest with the q slit design.

Although the proposed design technique has been demonstrated for a 12-slot/10-pole FSCW-IPM machine with SL windings, it can successfully be applied to other types of PM machines that have significant sub-harmonic MMF components.

Acknowledgment

This work was supported by Ford Motor Company, Ltd. The authors would like to thank JSOL Corporation, for the generous support, in making their JMAG finite-element software available.

References

[1] A. M. EL-Refaie, "Fractional-slot concentrated-windings synchronous permanent magnet machines: Opportunities and challenges," *IEEE Trans. Ind. Electron.*, vol. 57, no. 1, pp. 107–121, Jan. 2010.

[2] K. Atallah, D. Howe, P. H. Mellor, and D. A. Stone, "Rotor loss in permanent-magnet brushless AC machines," *IEEE Trans. Ind. Appl.*, vol. 36, no. 6, pp. 1612–1618, Nov./Dec. 2000.

[3] G. Dajaku, W. Xie, and D. Gerling, "Reduction of low space harmonics for the fractional slot concentrated windings using a novel stator design," *IEEE Trans. Magn.*, vol. 50, no. 5, May 2014, Art. ID 8201012.

[4] L. Wu, R. Qu, and D. Li, "Reduction of rotor eddy-current losses for surface PM machines with fractional slot concentrated windings and retaining sleeve," *IEEE Trans. Magn.*, vol. 50, no. 11, Nov. 2014, Art. ID 8205704.

[5] P. B. Reddy, A. M. EL-Refaie, and K.-K. Huh, "Effect of number of layers on performance of fractional-slot concentrated-windings interior permanent magnet machines," *IEEE Trans. Power Electron.*, vol. 30, no. 4, pp. 2205–2218, Apr. 2015.

[6] L. Alberti, E. Fornasiero, and N. Bianchi, "Impact of the rotor yoke geometry on rotor losses in permanent-magnet machines," *IEEE Trans. Ind. Appl.*, vol. 48, no. 1, pp. 98–105, Jan./Feb. 2012.

[7] N. Bianchi, M. D. Prè, L. Alberti, and E. Fornasiero, *Theory and Design of Fractional-Slot PM Machines*. Padova, Italy: CLEUP, Sep. 2007.

[8] S.-H. Han, T. M. Jahns, and Z. Q. Zhu, "Analysis of rotor core eddy-current losses in interior permanent-magnet synchronous machines," *IEEE Trans. Ind. Appl.*, vol. 46, no. 1, pp. 196–205, Jan./Feb. 2010.

[9] K. Yamazaki and Y. Fukushima, "Effect of eddy-current loss reduction by magnet segmentation in synchronous motors with concentrated windings," *IEEE Trans. Ind. Appl.*, vol. 47, no. 2, pp. 779–788, Mar./Apr. 2011.